



ARTICLE

DOI: 10.1038/s41467-018-04613-x

OPEN

Live cyanobacteria produce photocurrent and hydrogen using both the respiratory and photosynthetic systems

Gadiel Saper¹, Dan Kallmann¹, Felipe Conzuelo², Fangyuan Zhao², Tünde N. Tóth^{1,3}, Varda Liveanu⁴, Sagit Meir⁵, Jędrzej Szymanski^{5,6}, Asaph Aharoni⁵, Wolfgang Schuhmann ², Avner Rothschild^{1,7}, Gadi Schuster^{1,4} & Noam Adir ^{1,3}

Oxygenic photosynthetic organisms perform solar energy conversion of water and CO₂ to O₂ and sugar at a broad range of wavelengths and light intensities. These cells also metabolize sugars using a respiratory system that functionally overlaps the photosynthetic apparatus. In this study, we describe the harvesting of photocurrent used for hydrogen production from live cyanobacteria. A non-harmful gentle physical treatment of the cyanobacterial cells enables light-driven electron transfer by an endogenous mediator to a graphite electrode in a biophotocatalytic cell, without the addition of sacrificial electron donors or acceptors. We show that the photocurrent is derived from photosystem I and that the electrons originate from carbohydrates digested by the respiratory system. Finally, the current is utilized for hydrogen evolution on the cathode at a bias of 0.65 V. Taken together, we present a biophotocatalytic system where live cyanobacteria produce stable photocurrent that can generate hydrogen.

¹The Nancy & Stephen Grand Technion Energy Program (GTEP), Technion – Israel Institute of Technology, Technion City, 32000 Haifa, Israel. ²Analytical Chemistry – Center for Electrochemical Sciences (CES), Ruhr-Universität Bochum, Universitätsstr. 150, 44780 Bochum, Germany. ³Schulich Faculty of Chemistry, Technion – Israel Institute of Technology, Technion City, 32000 Haifa, Israel. ⁴Faculty of Biology, Technion – Israel Institute of Technology, Technion City, 32000 Haifa, Israel. ⁵Department of Plant and Environmental Sciences, The Weizmann Institute of Science, Rehovot, Israel. ⁶Leibniz Institute of Plant Genetics and Crop Research (IPK), Network Analysis and Modelling, OT Gatersleben, 06466 Seeland, Germany. ⁷Department of Materials Science and Engineering, Technion – Israel Institute of Technology, Technion City, 32000 Haifa, Israel. These authors contributed equally: Gadiel Saper, Dan Kallmann. Correspondence and requests for materials should be addressed to G.S. (email: gadis@technion.ac.il) or to N.A. (email: noam@ch.technion.ac.il)

Cyanobacteria are a wide class of photosynthetic organisms that have been recently proposed as potential sources of materials (membranes, complexes) from which photo-excited electrons can be extracted to produce electrical current and renewable fuels^{1–3}. Different species of cyanobacteria living in a wide range of habitats, were responsible for the original formation of the Earth's oxygen enriched atmosphere, and continue to serve as a major source of primary production and oxygen evolution⁴. In cyanobacterial photosynthesis, the major photosynthetically relevant light absorbing pigment is chlorophyll (chl) *a*, which has maximal absorbance at 420–460 nm and 670–700 nm. The phycobilisome (PBS) antenna complex additionally absorbs between 550–680 nm. Photosystem I (PSI) also contains a minor antennae complex that has been shown to be red-shifted to ~710–730 nm^{5–8}. The energy is efficiently transferred from the antennas to the Photosystem II (PSII) and PSI reaction centers (P₆₈₀ and P₇₀₀, respectively)^{9–11}. In this light-driven process, electrons from water are sequentially transferred through a series of redox species to finally reduce NADP⁺ to be used for carbon fixation^{12,13} (Fig. 1). A proton-motive gradient is created between the thylakoid membrane lumen and the cytoplasm, resulting in proton-coupled electron transfer, which serves as the driving force for ATP production.

In the dark, cyanobacterial cells oxidize carbon sources via the respiratory system. For example, glucose is oxidized to acetyl CoA in the glycolytic process. Acetyl CoA is further oxidized in the tricarboxylic acid (TCA) cycle. These processes produce ATP, NADH, and FADH₂. NADH and FADH₂ are oxidized during

oxidative phosphorylation to consume oxygen and produce CO₂ and ATP^{14–16}. Cyanobacteria lack the separation afforded by eukaryotic organelles, and it has been previously shown that electrons can flow between the photosynthetic and respiratory systems via redox active molecules¹⁷. For example, quinones from the photosynthetic plastoquinone (PQ) pool can oxidize NADH and FADH₂, both products of glucose oxidation^{17–21} (Fig. 1).

Various attempts have been made to extract electrons from photosynthetic systems for the purpose of solar energy conversion (SEC)^{19,22–29}. In some studies, isolated photosystems (PS) have been used within a bio-photoelectrochemical cell (BPEC) to produce electric power^{30–34}. With isolated PS, an exogenous electron acceptor has to be used as a mediator (when utilizing PSI or bacterial reaction centers, an exogenous donor is also required) and the PS has to be fixed to the electrode, for instance by the presence of an immobilized mediator or a redox polymer^{24,25,31,34}. In the case of PSII, water can serve as the electron donor, dependent on the stability of the oxygen evolving complex (OEC). One of the main problems with using isolated photosynthetic complexes for SEC is the relatively short lifetime of the biological components of the system, due to damage caused by radicals formed within the reaction centers^{35,36}. Combined membrane systems have an evolutionary benefit for energy conversion that has recently been identified as a characteristic that could improve artificial photosynthetic SEC systems³⁵. The use of living cells could mitigate this problem due to the presence of repair systems that can replace photo-damaged photosynthetic proteins. However, extracting electrons from living organisms is potentially more complicated as it may require an exogenous electron carrier (mediator) that can penetrate the cell wall and membrane, such as ferricyanide, cytochrome, or 2,6-dichloro-1,4-benzoquinone (DCBQ)^{23,27,36–39}. To overcome this difficulty, cyanobacterial cells have been grown or dried on an electrode to extract an electric current by direct contact^{1,28,40,41}. However, when such direct contact is utilized, the electric current is limited, as it will likely be generated from only a single layer of cells.

Here, we describe the construction of a BPEC in which live cyanobacteria produce a significant photocurrent that is derived from electrons of the respiratory and photosynthetic systems, without the need for exogenous electron donors or mediators. The resulting current was utilized for the production of molecular hydrogen on the cathode at a bias voltage of 0.65 V.

Results and Discussion

Production of a significant current by living cells. Cyanobacterial cells, *Synechocystis* sp. PCC 6803, were gently treated with a microfluidizer (herein called iSyn, see methods), and applied by gravity onto the graphite electrode. A platinum wire serves as the cathode while an Ag/AgCl/3 M NaCl electrode is used as a reference in all measurements (BPEC, Fig. 2a). When we measured current over time (chronoamperometry, CA), at an applied potential of 150 mV (vs. Ag/AgCl/3 M NaCl) (standard working potential obtained from the IV curve (Supplementary Fig. 1A), for all CA experiments unless mentioned otherwise), a dark current of $5 \pm 1 \mu\text{A cm}^{-2}$ was obtained, probably directly from the respiratory system, as previously suggested^{36,37} (Fig. 2b, initial 100 seconds). Upon illumination, the current increased to the maximum stable current of $36 \pm 4 \mu\text{A cm}^{-2}$. Accordingly, the net produced photocurrent was $31 \pm 4 \mu\text{A cm}^{-2}$. Upon return to dark, there was a slow decline in the measured current. We noticed that the addition of the photosynthetic electron flow inhibitor, 3-(3,4-dichlorophenyl)-1,1-dimethylurea (DCMU), resulted in a significantly faster increase in the photocurrent, reaching the maximum value in about 3 min, as compared to about 13 min in the absence of DCMU (Fig. 2b). Thus, DCMU

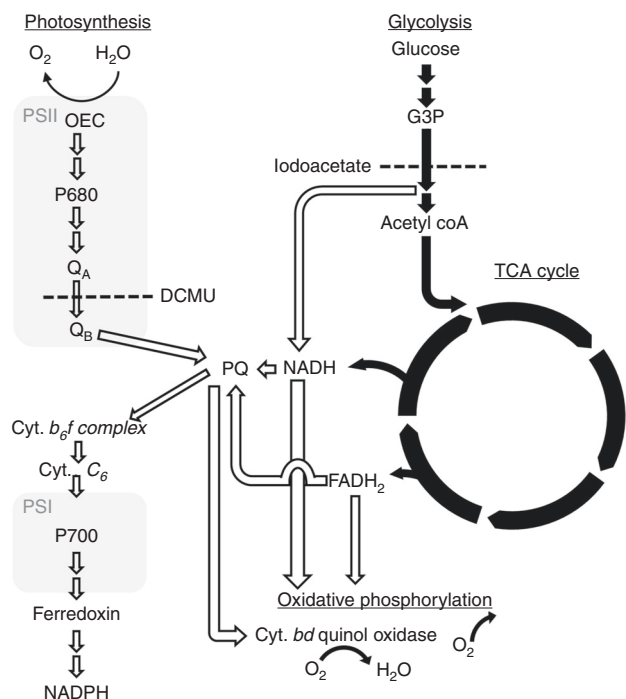


Fig. 1 The electron flow of the photosynthetic process and respiration metabolism in cyanobacteria. The scheme was drawn based on the data described in references 12–21. Filled black arrows mark the respiration metabolism. Unfilled arrows indicate the photosynthetic and additional electron flow processes. Double arrows mark additional steps not shown for clarity. G3P is glyceraldehyde 3 phosphate, and TCA stands for tricarboxylic acid cycle. The membrane soluble plastoquinone (PQ) functions as an acceptor of residual electrons of the glycolysis and the TCA cycle, as well as an essential mediator of the photosynthetic electrons between PSII and the *b₆f* complex. Dashed lines indicate the site of action of inhibitors of the photosynthetic or respiratory, used in this work

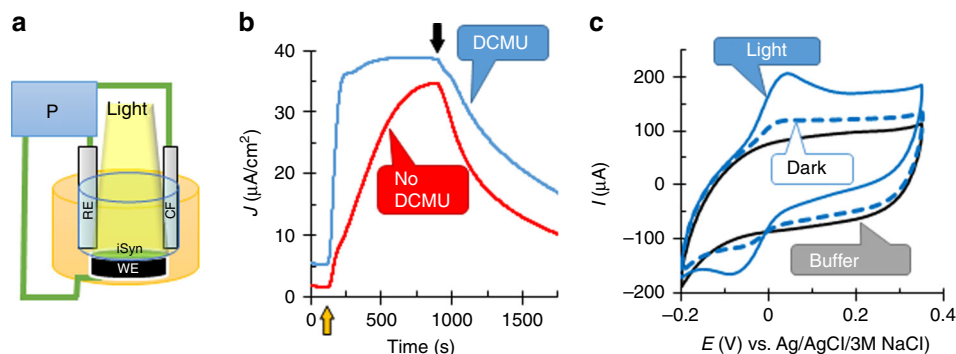


Fig. 2 Gently treated *Synechocystis* cells generate an enhanced photocurrent using an endogenous redox mediator. **a** Schematic drawing of the bio photoelectrochemical apparatus with the *iSyn* settled on the working electrode (WE). The counter electrode (CE) is platinum, and the reference electrode (RE) an Ag/AgCl/3 M NaCl. All electrodes are connected to the potentiostat (P). **b** Chronoamperometric measurements at 150 mV (vs. Ag/AgCl/3 M NaCl) for *iSyn* in the presence (blue) or absence (red) of DCMU. The yellow up arrow indicates light on (the initial 100 seconds show the dark current) and the black down arrow indicates light off. **c** Cyclic voltammograms of *iSyn*, illuminated (solid blue lines) or in the dark (dashed blue lines). Buffer lacking *iSyn* shows no redox activity (black solid line). Measurements recorded at a rate of 5 mV s^{-1}

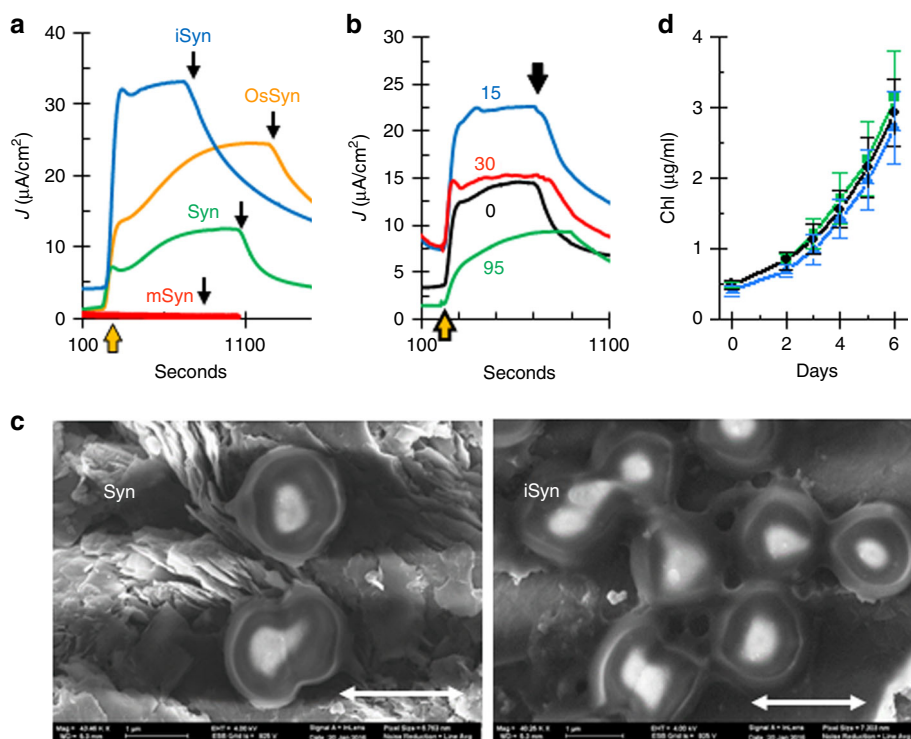


Fig. 3 *iSyn* are living, modified, and clustered cells. **a** CA measurements of *Synechocystis* cells (*Syn*, green), cells undergone a mild osmotic shock treatment (*OsSyn*, Orange), cells undergone a gentle pressure treatment (*iSyn*, blue), and thylakoid membranes (*mSyn*, red). **b** CA measurements of cell undergone treatment with microfluidizer at 0, 15, 30, and 95 psi, as indicated in the figure. **c** SEM image of *iSyn* (right) and *Syn* (left) on graphite. Scale bars are 2 μm . **d** Growth curve of *Syn* (green), *iSyn* (black) and *iSyn* that were illuminated for 30 min in the BEPC (blue) in liquid medium. The vertical lines show the standard deviation ($n = 5$)

was used for all electrochemical measurements unless mentioned otherwise. Cyclic voltammetry (CV) of the *iSyn* indicated the presence of a redox active species with an anodic peak at 50 mV (vs. Ag/AgCl/3 M NaCl) and a cathodic peak at -70 mV (vs. Ag/AgCl/3 M NaCl). The anodic current was significantly increased during illumination to present a quasi-reversible voltammogram, suggesting a photo-induced catalytic reaction mediated by a redox species (Fig. 2c). Optimization experiments show that increasing the amount of cells increases both CV (Supplementary Fig. 1B) and CA (Supplementary Fig. 1C) values up to a plateau of 150–225 μg chlorophyll. Since no external mediating electron transfer molecules were added to the BPEC, we conclude that the

source of the redox species identified in Fig. 2c is from within the *Syn* cells. The characterization of this mediator will be described in detail below.

We noticed that there was a negative correlation between the pressure used during the treatment performed on the cells and the measured current (Fig. 3a). The highest current was obtained when the lowest possible pressure of the microfluidizer was used (Fig. 3b). Lower currents were obtained when using untreated cells (*Syn*) or cells that were osmotically shocked (*OsSyn*). Membrane fragments obtained from cells that were completely disrupted at higher pressure with a French Pressure cell (*mSyn*) did not produce measurable currents (Fig. 3a). The

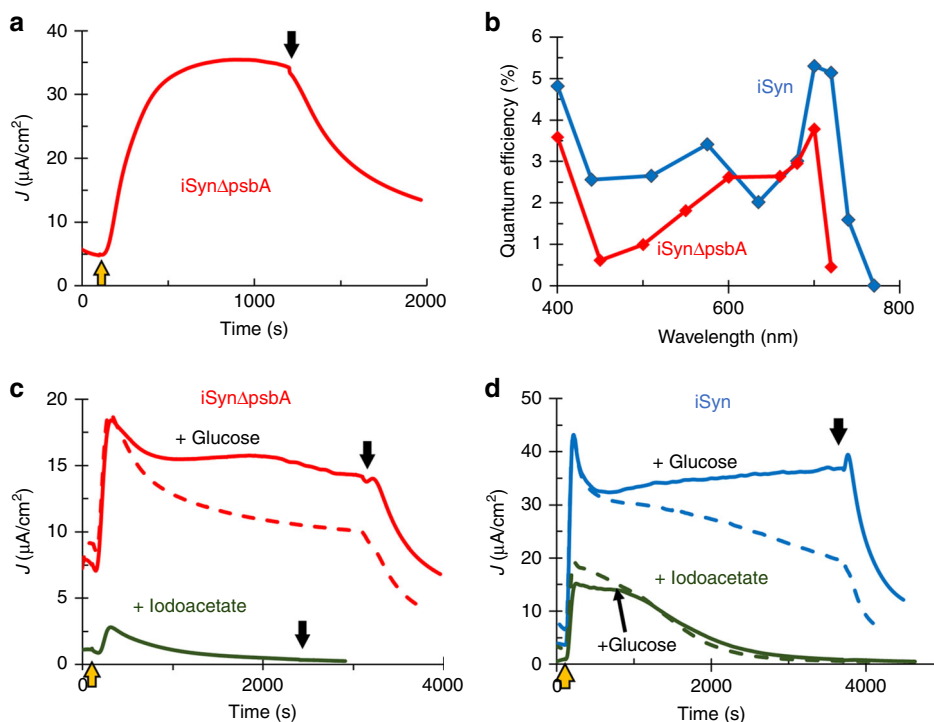


Fig. 4 iSyn photocurrent to the BPEC involves both photosynthetic and respiratory systems. **a** CA measurements for iSyn Δ psbA. **b** Action spectra: the obtained photocurrent was normalized to the photon energy input (external quantum efficiency) at different wavelengths. The external quantum efficiency of iSyn is shown in blue and that of iSyn Δ psbA in red. A new measurement with fresh cells was used for each wavelength. **c** CA measurements for iSyn Δ psbA without (red) and with (green) the addition of iodoacetate and in the presence (full line) or absence (dashed line) of glucose. **d** CA measurements for iSyn without (blue) and with (green) the addition of iodoacetate or in the presence (full line) or absence (dashed line) of glucose in the buffer

microfluidizer treatment (iSyn) resulted with a higher anodic peak in the dark, compared to OsSyn and Syn (Supplementary Fig. 1D), whereas membrane fragments did not show any anodic peak (Supplementary Fig. 1E) indicating the absence of the redox species (see methods for all preparations). iSyn appear to retain their cellular structure and remain clumped together as visualized by scanning electron microscopy (SEM) and fluorescent microscopy (Fig. 3c, Supplementary Fig. 2A, respectively). To further investigate the state of the iSyn preparation, we utilized confocal fluorescence microscopy. Syn, OsSyn, and iSyn appeared in the microscope to retain PBS functional integrity. Treatment of the same cells using higher pressures (mSyn) produces aggregated membranous material, lacking the PBSs (Supplementary Fig. 2A–C), which are soluble and spontaneously released from the membranes⁹. The major difference between the Syn and iSyn is that the latter are clumped together in large clusters (Fig. 3c, Supplementary Fig. 2A). In the OsSyn preparation, cells are seen to form smaller clusters of two or three cells with the same appearance of fusion (Supplementary Fig. 2A). To determine cell viability, we prepared cells as described above, and illuminated them for 30 min in the BPEC under standard conditions. We then removed the iSyn from the BPEC by simple washing. The growth rate of the iSyn was then compared to the growth rates of either untreated Syn or non-illuminated iSyn in new growth media. All cells had similar growth rates (Fig. 3d and Supplementary Fig. 3a). To further determine cell viability, we performed a colony formation test (Supplementary Fig. 3B). We applied an amount of Syn, iSyn, or membranes (mSyn) containing the same amount of chlorophyll onto a growth plate, and followed the growth of the colonies. Syn and iSyn grow at a similar rate, 364 ± 98 and 280 ± 68 colonies per femtograms of *Chl a* to Syn and iSyn, respectively, whereas mSyn contains much smaller amount of living cells (11 ± 3). These results indicate that

the application of mild pressure did not harm the ability of *Synechocystis* cells to multiply and divide. iSyn were also shown to photosynthetically evolve O_2 at a similar rate to Syn cells (O_2 evolution of 392 ± 53 , 464 ± 60 nmol O_2 μg chl⁻¹ h⁻¹ for iSyn and Syn, respectively). We thus suggest that iSyn are living, yet modified and/or clustered cells and that the change that occurs to the cells does not modify the biological energy transducing systems.

The combined activity of two pathways generates the current.

The photocurrent in the presence of DCMU could be explained by two alternative pathways. In the first one, the electrons are derived from water oxidation and are transferred to putative endogenous mediator(s) prior to Q_B , before the binding site of DCMU at Q_B , similar to the electron transfer from PSII to silicomolybdate^{42,43}. The second possibility is that DCMU inhibits the activity of PSII, including the water oxidation complex. In such a case, a light-driven electron source must be located further downstream of the Q_B site, and could involve the PQ pool, cytochrome *b₆f*, and finally PSI, as the site of photoactivity. A stable photocurrent that is not a result of PSII activity can only exist if there is an alternative source of electrons to PSI. Such a possible source could be the respiratory system that is linked to the photosynthetic apparatus in cyanobacteria^{14,17–21} (Fig. 1). To differentiate between these possibilities we repeated the electrochemical experiments with a non-autotrophic mutant of *Synechocystis* sp. PCC 6803, where the *psbA* genes (encoding the D1 protein) have been deleted, thus leading to a non-functional PSII (Δ psbA)^{43,44} (Supplementary Fig. 4A). CA measurements displayed a photocurrent that is similar to that obtained with iSyn (Fig. 4a). Moreover, the iSyn Δ psbA cells look similar to iSyn cells (Supplementary Fig. 4B) and require the same preparation for

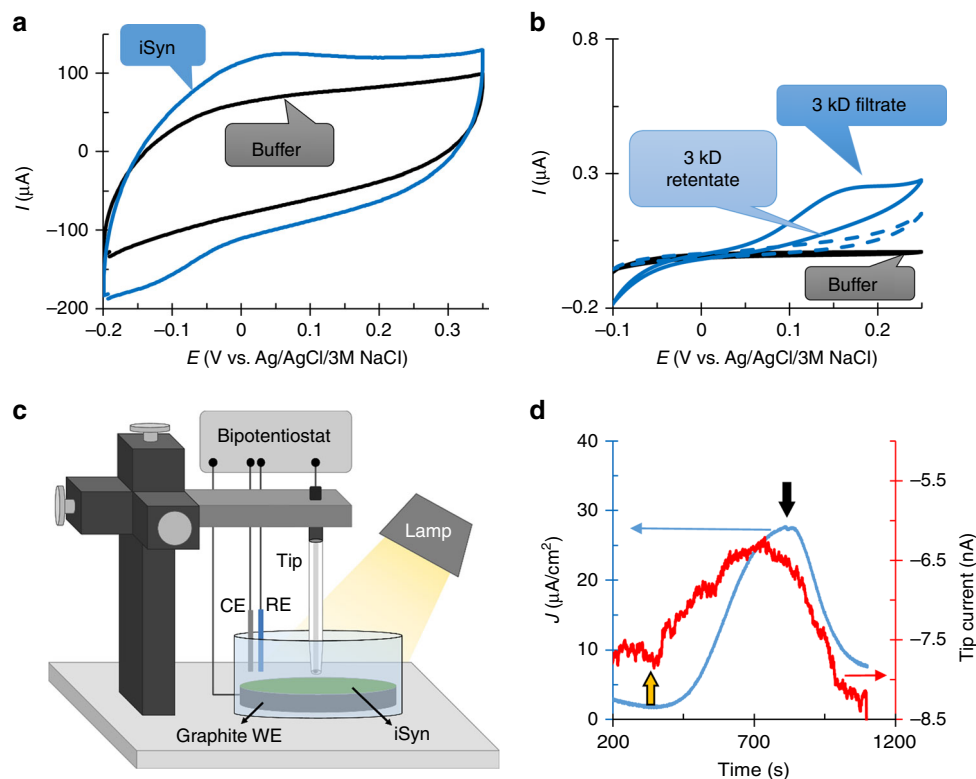


Fig. 5 iSyn electron transfer to the BPEC is via a diffusive endogenous mediator. **a** CV in the light for buffer (black) and the iSyn (blue) separated by a 3 kD dialysis membrane on the graphite electrode. **b** CV of supernatant fraction from centrifuged iSyn cells separated by filtration through 3 kD cut-off centricron. Filtrate (solid blue line), retentate (dashed blue), and buffer (black). **c** Illustration of the scanning electrochemical microscopy setup. iSyn settled on the working electrode (WE) electrode. The counter electrode (CE) is platinum, and the reference electrode (RE) a Ag/AgCl/3 M KCl. The tip is a carbon-based microelectrode with a mixture of bilirubin oxidase (BOD) embedded in an Os-complex modified polymer matrix. All electrodes are connected to the bipotentiostat. **d** CA of the iSyn (blue) and the BOD tip current (red) measuring the oxidation of the mediator at a distance of 30 μm from the graphite electrode

optimal photocurrent as iSyn does (Supplementary Fig. 4B–D). The iSyn Δ psbA cells also contain the same redox mediator (Supplementary Fig. 4D). Another proof of the lack of involvement of PSII in the electron transfer pathway in the BPEC was to inactivate the OEC of PSII by incubation with Tris buffer. In the Tris treated iSyn similar photocurrents were obtained (Supplementary Fig. 5A–B). Taken together these results indicate that the electron path is from the respiratory system, through PSI and to the electrode.

To further support the notion that the photosystem deriving the photocurrent is PSI and not PSII, we measured the action spectrum of the photocurrent production. To this end, we measured the photocurrent as a function of the wavelength and calculated the external quantum efficiency (EQE) at each wavelength (Fig. 4b). The EQE in both iSyn and iSyn Δ psbA was evident at all wavelengths of visible light with an increase at 700 nm suggesting the importance of the participation of PSI in the activity. Together, these results demonstrated that PSI and not PSII is the photosystem that drives the photocurrent when iSyn cells are illuminated in the BPEC.

As already indicated above, the lack of the water oxidation activity of PSII in the iSyn Δ psbA indicates that there must be an alternative electron donor. Studies suggest that electron transfer between the respiratory system and the photosynthetic system may occur via the plastoquinone (PQ) pool^{14,18}. To investigate this, we performed experiments in the presence of glucose. Glucose is known to be uptaken by *Synechocystis* cells, providing energy for growth in the dark or for growth of non-photosynthetic mutants^{43,44}. Addition of glucose significantly

extended the period of the production of the highest current (Fig. 4c). Furthermore, iodoacetate, which blocks the respiratory path at the site of glyceraldehyde-3-phosphosphate dehydrogenase activity (Fig. 1), significantly inhibited the photocurrent (Fig. 4c), supporting the suggestion that the respiratory system is the main electron donor.

The above measurements support our hypothesis that under these conditions a respiratory-PSI electron transfer pathway exists in the Δ psbA mutant. In a fashion similar to that seen for iSyn Δ psbA, iSyn also exhibits extended photocurrent lifetime in the presence of glucose (Fig. 4d and Supplementary Fig. 5C–D), and the photocurrent is decreased in the presence of iodoacetate (Fig. 4d), reaffirming that the major electron source is the respiratory system. Together, the results so far uncover an electron transfer pathway in which electrons derived from the respiratory pathway reduce PSI that can further photo-reduce the electrode in the gently treated *Synechocystis* live cells.

The mediator is a small diffusive soluble molecule. Electrochemical experiments show a slow increase and slower decline in the photocurrent (Fig. 2b). Moreover, the potential difference between the anodic and cathodic peaks in the voltammogram (Fig. 2c) suggests that the current in the BPEC is mediated by a diffusive soluble molecule. Cyanobacterial cells contain both small redox active proteins, as well as metabolites that undergo redox reactions. We introduced a single layer synthetic membrane with a nominal molecular weight cut-off of 3 kD between the iSyn and the electrode (Fig. 5a) and performed CV

measurements under light. These show the same anodic and cathodic peaks in the presence of iSyn as without the membrane, suggesting the mediator can diffuse through a 3-kD membrane and is thus most likely not a protein.

To further isolate the mediator, iSyn were illuminated followed by centrifugation. The supernatant was then filtered through a 3 kD ultrafiltration device and CV measurements were performed on both the filtrate and retentate. These measurements show that only the filtrate contains a redox active species while the retentate has no redox active component (Fig. 5b). This indicates that the mediator is a water-soluble molecule that passes through the 3-kD filter. Similar experiments performed on dark exposed iSyn (Supplementary Fig. 6A) showed the presence of a redox peak but with a smaller area, suggesting that illumination increases the release of the mediator from the cells. In addition, the redox behavior of the mediator is inactivated after 10 min incubation at 60 °C (Supplementary Fig. 6B). We suggest that the redox molecules could be a soluble quinone, a flavonoid^{44,45} or a small peptide that is temperature sensitive.

Scanning electrochemical microscopy (SECM) was used to exclude the possible release of O₂ under irradiation and proved the existence of a soluble mediator in accordance with the CA measurements. SECM measures the local current on a micro-electrode tip precisely positioned above the evaluated sample. SECM can be used to measure local electrochemical reactions over an evaluated sample or to efficiently collect reaction products with the tip placed in close proximity to the analyzed surface, for example, it was previously used to measure oxygen production by n-type semiconductor-based photo-anodes for water splitting^{45,46}. The SECM experiment was performed by placing the tip microelectrode above the center of the cells at ~30 μm from the graphite electrode surface with iSyn deposited on top (Fig. 5c). As SECM probe we used a carbon-based microelectrode modified with bilirubin oxidase (BOD) embedded in an Os-complex modified polymer matrix^{47,48}. The electrode was polarized at 0 mV (vs. Ag/AgCl/3 M KCl) for the steady-state reduction of O₂. To decrease the background current related with the reduction of O₂ naturally present in solution, Ar was bubbled into the buffer for 15 min before the measurement and continuously, gently, bubbled during the measurement. The obtained results in the SECM measurements clearly demonstrate the absence of any cathodic current related to the collection of O₂ evolved from the sample. Furthermore, a considerable shift in the recorded current at the microelectrode toward more positive values was observed under irradiation and following a clear correlation between the sample current and the tip current under dark and light conditions (Fig. 5d). The shift in current at the SECM probe can then be attributed to the oxidation of the soluble mediator at the tip microelectrode that is polarized at a more negative potential than the redox peak observed for the mediator in previous experiments (Fig. 2c). Further measurements at a tip potential of -200 mV (vs. Ag/AgCl/3 M KCl) indicate a reduction of the mediator in the light (Supplementary Fig. 6C). SECM measurements confirmed that the mediator diffuses from the iSyn through the solution to the tip. Thus, we can conclude that there is a water-soluble electron carrier that mediates between the iSyn and the electrode.

Finally, in an attempt to identify the electron carrier mediator if it is a metabolite, we carried out a metabolic profiling^{49,50} of Syn, iSyn, and iSyn that were illuminated in the BEPC. No significant change between the different samples profile was detected, suggesting that the gentle treatment does not cause a significant change in the amount of a metabolite but rather the release of the mediator to the medium or the outtrace of the cells (Supplementary Fig. 7 and Supplementary Table 2).

DCMU has a unique effect in the iSyn BPEC. In the presence of DCMU, the maximum current is reached faster and the current is slightly enhanced (Fig. 2b, Supplementary Fig. 8A,B). However, the photocurrent lifetime is prolonged by the presence of added glucose in either the presence or absence of DCMU (Supplementary Fig. 8C), suggesting that DCMU affects the electron flow but not the stability of the photocurrent. Counter-intuitively, the presence of DCMU was found to be crucial for the photocurrent production by the iSynΔpsbA, since in the absence of DCMU the photocurrent drops to 14% of the photocurrent obtained in the presence of DCMU (Supplementary Fig. 8B,D). Thus, even though iSynΔpsbA lacks the well-studied PSII-binding-site of DCMU, the addition of the herbicide has a dramatic effect and actually was essential for the production of the 20–30 μA cm⁻² current obtained with iSynΔpsbA even without DCMU (Supplementary Fig. 8D). The effect of DCMU in the iSynΔpsbA strongly indicates that DCMU has secondary binding sites with *Synechocystis* cells that have not yet been characterized. Moreover, DCMU increase the release of the mediator (Supplementary Fig. 8E) and as a results increases the photocurrent and decreases the time it takes to reach the maximum photocurrent (Fig. 2b, Supplementary Fig. 8C). Our results suggest that DCMU affects the production of the photocurrent in both iSyn and iSynΔpsbA at secondary site(s) by either inhibiting forward electron flow within the respiratory system, or by enhancing the release of the mediator.

Hydrogen is produced in the BPEC. As no external redox components were added to the BPEC, we presumed that protons are reduced to molecular hydrogen at the Pt cathode. To measure hydrogen production, we built a gas-tight BPEC connected directly to a gas-chromatograph (GC) (Fig. 6a). The gas actively diffuses via ducts and is pumped into the GC, hence there is a short delay in the gas measurement. Figure 6b shows the H₂(g) production over time measured using this configuration applying a voltage of 650 mV between the anode and cathode. The lack of H₂(g) production in the absence of light and/or iSyn (Supplementary Table 1) indicates a correlation between the light-current and the H₂ production. During the 2 h of illumination an average of 3.5 μmol H₂(g) mg Chl⁻¹ h⁻¹ is produced at a Faradaic efficiency of ca. 36%. The low Faradaic efficiency is most likely the result of molecular oxygen in the buffer, indicated by higher Faradaic efficiency in the absence of oxygen (Supplementary Fig. 9), or the mediator reduced on the cathode in addition to proton reduction.

In this study, we show light-driven current and hydrogen production with mildly treated live *Synechocystis* sp. PCC 6803 on a graphite electrode. The simple treatment makes the electron transfer possible from the cells to the electrode. This is the first time CV measurements indicate the existence of an endogenous mediator that can exit the cells' membranes in mildly treated live cyanobacteria^{50,51}. The electron extraction, by the intrinsic mediator, is photo-driven by PSI (Fig. 6c) that is reduced by the respiratory system, explaining the enhancing effect of glucose addition. In the absence of externally added glucose, the current originates from the internal carbohydrate pool produced during the growth phase. Whether PSI reduces the mediator directly or through other components of the photosynthetic electron transfer chain has not yet been ascertained. It is important to note that current is obtained from non-treated cells as well, however at much lower rates. This reiterates that the role of the treatment is to augment the amount of released mediator, and not the inducing of any modification to either of the two biological systems. During the review process of this article, a manuscript suggesting mediator dependent electron transfer in cyanobacteria

Technion) using a Zennium electrochemical workstation (*Zahner Elektrik*) and a solar simulator light source (*Oriel Sol3A*), or at the Hydrogen Lab (Grand Technion Energy Program) with an nStat multichannel potentiostat (*Ivium*) and a Xenon lamp solar simulator (*Abet*). For some measurements, we used a Palmsens3 (*Palmsens*) potentiostat and A1 light line (*Sciencetech*). All measurements were carried out in a three electrodes configuration under the illumination of one solar unit (1SU). Graphite (*Graphite Store*, *pn#bl001230*) was used as a working electrode, a Pt electrode (*ALS*) served as the counter electrode and a Ag/AgCl/3 M NaCl as a reference electrode (*ALS*). For each measurement, a sample containing 150 µg of chl *a* was placed on the 1.8 cm diameter graphite electrode. The sample was not stirred or replaced during the measurement. The medium was phosphate buffer (100 mM phosphate, pH 6) containing 100 mM NaCl. When indicated, 150 µM of DCMU was added. For the *ΔpsbA* mutant, chlorophyll amount of 50 µg was used. For the relevant electrochemical measurements, 6 mM of D-glucose in the absence or presence of 5 mM iodoacetic acid (sodium salt) were added.

Quantum efficiency measurements. The EQE of the BPEC containing iSyn (150 µg chl) was measured at a potential of 150 mV (vs. Ag/AgCl/3 M NaCl). The iSyn cells were illuminated with monochromatic light obtained by coupling a white light source to a monochromator (Cornerstone CS260) with a spectral bandwidth of 10 nm. Fresh cells were used in each measurement, and the maximum photocurrent was recorded. The photon flux was obtained from the light intensity measured by a power meter (918D High Performance Photodiode Sensor), and the EQE was calculated according to equation 1:

$$\text{EQE} = \frac{\text{Maximum photocurrent} / q}{\text{Photon flux}} \quad (1)$$

where q is the electron charge.

When analyzing iSyn Δ psbA we used 50 µg chl for each measurement and the bandwidth was 20 nm.

Oxygen evolution measurements. For measurement the photosynthetic activity by analyzing the rate of oxygen evolution, the cells (10 µg chl *a*) were placed in phosphate buffer (pH 6) in a final volume of 1 ml. A volume of 3 mM 2,6-dichloro-1,4-benzoquinone (DCBQ) was used as an electron acceptor and oxygen evolution was determined using a Clark-type electrode (*Hansatech*). Following preincubation in the dark for 2 min, the cells were illuminated with a white light halogen projector lamp (*MRC*) for 1 min and the increase in oxygen concentration was digitally measured.

Gas chromatography experiments. Hydrogen measurements were performed in the Hydrogen Lab (Grad Technion Energy Program) using an Agilent 7890 A GC system (*Agilent technologies*) with a molsieve 5 Å column, 10 ft*1/8"*2 mm (*Agilent technologies*) to determine H₂ production. Gas from the BPEC was continuously pumped to the GC. The applied potential on the working electrode was 50 mV (vs. Ag/AgCl/3 M NaCl). The bias between the anode and cathode measured by a voltmeter (m832, *Mastech*) was 650 mV. Calibration was performed by measuring known amounts of hydrogen directly injected to the GC.

Scanning electron microscopy. The morphology of cellular samples was characterized by high-resolution scanning electron microscopy (SEM) (Ultra PLUS, *Zeiss*). Further experimental details are found in the figure legend.

Purification of the mediator. iSyn cells, correspond to 400 µg chlorophyll from the stock solution, were illuminated for 5 min (without DCMU) in a 1.5 ml tube and then centrifuged (5417 R, *Eppendorf*) for 1 min at max speed. The supernatant was collected, the pellet was resuspended in 250 µl Phosphate buffer, centrifuged again, and the supernatant was collected. Filtration was performed using 3 kD (*Vivaspin 500*, *Sartorius Stedim biotech*) and centrifugation (5417 R, *Eppendorf*) for 1 h at 14,000× *g*. Heat inactivation was performed in a block heater (*SKS Biomedical instruments*) at 60 °C for 10 min.

Scanning electrochemical microscopy. SECM experiments were performed using a Ag/AgCl/3 M KCl double junction reference electrode, a Pt cylindrical mesh as counter electrode, and a BOD modified carbon microelectrode as electrochemical probe. The BOD modified tip was fabricated following a previously reported procedure^{54,55} by modifying a carbon-based microelectrode with a mixture of BOD embedded in an Os-complex modified polymer matrix^{47,48}. The SECM setup is schematically shown in Fig. 5c and is based on a previously described system^{46,47} consisting of three stepmotor driven micrometer screws (*Owis*) for positioning of the SECM tip in *x*-, *y*-, and *z*-directions, a bipotentiostat (PGU-BI 100, *Jaissle*), and a control software programmed using Visual Basic 6.0. A 150 W Hg-Xe lamp (LC8, *Hamamatsu photonics*) was used for irradiation of the sample at an incident light intensity of 55 mW cm⁻² (visible light). The sample was placed in a Teflon SECM cell sealed with an O-ring exposing an area of about 0.385 cm². The tip was positioned in close proximity (~30 µm) to the analyzed sample by recording *z*-approach curves in air-saturated buffer before adding the iSyn. The BOD modified tip was polarized at 0 or -200 mV (vs. Ag/AgCl/3 M KCl). During the

measurement, a given potential of 150 mV (vs. Ag/AgCl/3 M KCl) was applied to the sample. Both the tip and sample current were recorded during light and dark periods. For the SECM measurements, we used frozen/thawed iSyn cells. After preparation of the cells as described above, dimethyl sulfoxide was added to the cells, prior to flash-freezing in liquid nitrogen. iSyn was later thawed on ice and used for the SECM experiments.

Procedures for PBS spectroscopic measurements, confocal imaging, Tris treatment, colony formation test, and metabolomics profiling were detailed in Supplementary Methods.

Data availability. All data presented in this paper can be obtained from the corresponding authors upon reasonable request.

Received: 15 July 2017 Accepted: 4 May 2018

Published online: 04 June 2018

References

- McCormick, A. J. et al. Photosynthetic biofilms in pure culture harness solar energy in a mediatorless bio-photovoltaic cell (BPV) system. *Energy Environ. Sci.* **4**, 4699–4709 (2011).
- Kaiser, B. K. et al. Fatty aldehydes in cyanobacteria are a metabolically flexible precursor for a diversity of biofuel products. *PLoS ONE* **8**, e58307 (2013).
- Deng, M.-D. & Coleman, J. R. Ethanol synthesis by genetic engineering in cyanobacteria. *Appl. Environ. Microbiol.* **65**, 523–528 (1999).
- Whitton, B. A. *Ecology of Cyanobacteria II: Their Diversity in Space and Time*. (Springer, Germany, 2012).
- Szewczyk, S., Giera, W., D'Haene, S., van Grondelle, R. & Gibasiewicz, K. Comparison of excitation energy transfer in cyanobacterial photosystem I in solution and immobilized on conducting glass. *Photosynth. Res.* **132**, 111–126 (2017).
- Novoderezhkin, V. I. et al. Mixing of exciton and charge-transfer states in light-harvesting complex Lhc4. *Phys. Chem. Chem. Phys.* **18**, 19368–19377 (2016).
- Gobets, B., van Stokkum, I. H. M., van Mourik, F., Dekker, J. P. & van Grondelle, R. Excitation wavelength dependence of the fluorescence kinetics in photosystem I particles from *Synechocystis* PCC 6803 and *Synechococcus elongatus*. *Biophys. J.* **85**, 3883–3898 (2003).
- Brecht, M., Radics, V., Nieder, J. B., Studier, H. & Bittl, R. Red antenna states of photosystem I from *Synechocystis* PCC 6803. *Biochemistry* **47**, 5536–5543 (2008).
- Adir, N. Elucidation of the molecular structures of components of the phycobilisome: Reconstructing a giant. *Photosynth. Res.* **85**, 15–32 (2005).
- van Amerongen, H. & Croce, R. Light harvesting in photosystem II. *Photosynth. Res.* **116**, 251–263 (2013).
- Croce, R. & van Amerongen, H. Light-harvesting in photosystem I. *Photosynth. Res.* **116**, 153–166 (2013).
- Nelson, N. & Yocum, C. F. Structure and function of photosystems I and II. *Annual Review of Plant Biology* **57**, 521–565 (2006).
- Raven, J. A. & Beardall, J. In: P. A. del Giorgio, P. J. LeB. Williams Ed. by. *Respiration in aquatic photolithotrophs. Respir. Aquat. Ecosyst* (pp. 36–46. Oxford Univ. Press, New York, 2005).
- Vermaas, W. F. J. Photosynthesis and respiration in cyanobacteria. *Encycl. Life Sci.* 245–251 (2001).
- Osanaï, T. et al. Genetic engineering of group 2 σ factor SigE widely activates expressions of sugar catabolic genes in *Synechocystis* species PCC 6803. *J. Biol. Chem.* **286**, 30962–30971 (2011).
- Knoop, H. et al. Flux balance analysis of cyanobacterial metabolism: the metabolic network of *Synechocystis* sp. PCC 6803. *PLoS Comput. Biol.* **9**, e1003081 (2013).
- Bradley, R. W., Bombelli, P., Lea-Smith, D. J. & Howe, C. J. Terminal oxidase mutants of the cyanobacterium *Synechocystis* sp. PCC 6803 show increased electrogenic activity in biological photo-voltaic systems. *Phys. Chem. Chem. Phys.* **15**, 13611–13618 (2013).
- Lea-Smith, D. J., Bombelli, P., Vasudevan, R. & Howe, C. J. Photosynthetic, respiratory and extracellular electron transport pathways in cyanobacteria. *Biochim. Biophys. Acta (BBA) Bioenerg.* **1857**, 247–255 (2016).
- McCormick, A. J. et al. Biophotovoltaics: oxygenic photosynthetic organisms in the world of bioelectrochemical systems. *Energy Environ. Sci.* **8**, 1092–1109 (2015).
- Zhang, L. et al. Deletion of *Synechocystis* sp. PCC 6803 leader peptidase LepB1 affects photosynthetic complexes and respiration. *Mol. Cell. Proteom.* **12**, 1192–1203 (2013).
- Schmetterer, G., Alge, D. & Gregor, W. Deletion of cytochrome *c* oxidase genes from the cyanobacterium *Synechocystis* sp. PCC6803: Evidence for alternative respiratory pathways. *Photosynth. Res.* **42**, 43–50 (1994).

22. Larom, S. et al. The Photosystem II D1-K238E mutation enhances electrical current production using cyanobacterial thylakoid membranes in a bio-photoelectrochemical cell. *Photosynth. Res.* **126**, 161–169 (2015).
23. Pinhasi, R. I. et al. Hybrid bio-photo-electro-chemical cells for solar water splitting. *Nat. Commun.* **7**, 12552 (2016).
24. Zhao, F. et al. Light induced H₂ evolution from a biophotocathode based on photosystem I–Pt nanoparticles complexes integrated in solvated redox polymers films. *J. Phys. Chem. B* **119**, 13726–13731 (2015).
25. Efrati, A. et al. Assembly of photo-bioelectrochemical cells using photosystem I-functionalized electrodes. *Nat. Energy* **1**, 15021 (2016).
26. Gizzie, E. A. et al. Photosystem I-polyaniline/TiO₂ solid-state solar cells: simple devices for biohybrid solar energy conversion. *Energy Environ. Sci.* **8**, 3572–3576 (2015).
27. Sekar, N., Umasankar, Y. & Ramasamy, R. P. Photocurrent generation by immobilized cyanobacteria via direct electron transport in photo-bioelectrochemical cells. *Phys. Chem. Chem. Phys.* **16**, 7862 (2014).
28. Sekar, N., Jain, R., Yan, Y. & Ramasamy, R. P. Enhanced photo-bioelectrochemical energy conversion by genetically engineered cyanobacteria. *Biotechnol. Bioeng.* **113**, 675–679 (2016).
29. Sawa, M. et al. Electricity generation from digitally printed cyanobacteria. *Nat. Commun.* **8**, 1327 (2017).
30. Mershin, A. et al. Self-assembled photosystem-I biophotovoltaics on nanostructured TiO₂ and ZnO. *Sci. Rep.* **2**, 234 (2012).
31. Yehezkeili, O. et al. Integrated photosystem II-based photo-bioelectrochemical cells. *Nat. Commun.* **3**, 742 (2012).
32. Efrati, A., Tel-Vered, R., Michaeli, D., Nechushtai, R. & Willner, I. Cytochrome c-coupled photosystem I and photosystem II (PSI/PSII) photo-bioelectrochemical cells. *Energy Environ. Sci.* **6**, 2950–2956 (2013).
33. Li, J. et al. Integrating photosystem II into a porous TiO₂ nanotube network toward highly efficient photo-bioelectrochemical cells. *J. Mater. Chem. A* **4**, 12197–12204 (2016).
34. Zhao, F., Sliozberg, K., Rögner, M., Plumeré, N. & Schuhmann, W. The role of hydrophobicity of Os-complex-modified polymers for photosystem I based photocathodes. *J. Electrochem. Soc.* **161**, H3035–H3041 (2014).
35. Yao, D. C. I., Brune, D. C. & Vermaas, W. F. J. Lifetimes of photosystem I and II proteins in the cyanobacterium *Synechocystis* sp. PCC 6803. *FEBS Lett.* **586**, 169–173 (2012).
36. McCormick, A. J. et al. Hydrogen production through oxygenic photosynthesis using the cyanobacterium *Synechocystis* sp. PCC 6803 in a bio-photoelectrolysis cell (BPE) system. *Energy Environ. Sci.* **6**, 2682–2690 (2013).
37. Pinhasi, R. I. et al. Photosynthetic Membranes of *Synechocystis* or Plants Convert Sunlight to Photocurrent through Different Pathways due to Different Architectures. *PLoS ONE* **10**, e0122616 (2015).
38. Larom, S., Salama, F., Schuster, G. & Adir, N. Engineering of an alternative electron transfer path in photosystem II. *Proc. Natl Acad. Sci. USA* **107**, 9650–9655 (2010).
39. Calkins, J. O., Umasankar, Y., O'Neill, H. & Ramasamy, R. P. High photo-electrochemical activity of thylakoid–carbon nanotube composites for photosynthetic energy conversion. *Energy Environ. Sci.* **6**, 1891–1900 (2013).
40. Cereda, A. et al. A bioelectrochemical approach to characterize extracellular electron transfer by *Synechocystis* sp. PCC6803. *PLoS ONE* **9**, e91484 (2014).
41. Wei, X., Lee, H. & Choi, S. Biopower generation in a microfluidic bio-solar panel. *Sens. Actuators B Chem.* **228**, 151–155 (2016).
42. Yruela, I., Montoya, G., Alonso, P. J. & Picorel, R. Identification of the pheophytin-QA-Fe domain of the reducing side of the photosystem II as the Cu (II)-inhibitory binding site. *J. Biol. Chem.* **266**, 22847–22850 (1991).
43. Nixon, P. J., Metz, J. G., Roegner, M. & Diner, B. A. A *Synechocystis* PCC 6803 *psbA* deletion mutant and its Transformation with a *psbA* gene from a higher plant. In *Current research in photosynthesis* 471–474 (Springer, Germany, 1990).
44. Marsili, E. et al. Shewanella secretes flavins that mediate extracellular electron transfer. *Proc. Natl Acad. Sci. USA* **105**, 3968–3973 (2008).
45. Essmann, V. et al. In operando investigation of electrically coupling of photosystem 1 and photosystem 2 by means of bipolar electrochemistry. *Anal. Chem.* **89**, 7160–7165 (2017).
46. Conzuelo, F. et al. High-resolution analysis of photoanodes for water splitting by means of scanning photoelectrochemical microscopy. *Anal. Chem.* **89**, 1222–1228 (2017).
47. Badura, A. et al. Photo-induced electron transfer between photosystem 2 via cross-linked redox hydrogels. *Electroanalysis* **20**, 1043–1047 (2008).
48. Sokol, K. P. et al. Rational wiring of photosystem II to hierarchical indium tin oxide electrodes using redox polymers. *Energy Environ. Sci.* **9**, 3698–3709 (2016).
49. Treves, H. et al. Metabolic flexibility underpins growth capabilities of the fastest growing alga. *Curr. Biol.* **27**, 2559–2567 (2017). e3.
50. Schuergers, N., Werlang, C., Ajo-Franklin, C. M. & Boghossian, A. A. A synthetic biology approach to engineering living photovoltaics. *Energy Environ. Sci.* **10**, 1102–1115 (2017).
51. Zou, Y., Pisciotto, J. & Baskakov, I. V. Nanostructured polypyrrole-coated anode for sun-powered microbial fuel cells. *Bioelectrochemistry* **79**, 50–56 (2010).
52. Wenzel, T., Härtter, D., Bombelli, P., Howe, C. J. & Steiner, U. Porous translucent electrodes enhance current generation from photosynthetic biofilms. *Nat. Commun.* **9**, 1299 (2018).
53. Arnon, D. I. Copper enzymes in isolated chloroplasts. Polyphenoloxidase in *Beta vulgaris*. *Plant Physiol.* **24**, 1 (1949).
54. Zhao, F. et al. A novel versatile microbiosensor for local hydrogen detection by means of scanning photoelectrochemical microscopy. *Biosens. Bioelectron.* **94**, 433–437 (2017).
55. Chabi, S. et al. Membranes for artificial photosynthesis. *Energy Environ. Sci.* **10**, 1320–1338 (2017).

Acknowledgements

This work was funded by the I-CORE Program of the Planning and Budgeting Committee, the Israel Science Foundation (Grant No. 152/11), a grant from the transformative program of the US-Israel Binational Science Foundation (BSF grant No. 2011556), and a grant from the Deutsche Forschungsgemeinschaft (DIP project LU315/17-1). The results reported in this work were obtained using central facilities at the Technion's Photovoltaic Laboratory, supported by the Nancy & Stephen Grand Technion Energy Program (GTEP) and by the Russell Berrie Nanotechnology Institute (RBNI), and at the Technion's Hydrogen Technologies Research Laboratory (HTRL), supported by the Adelis Foundation and by the Solar Fuels I-CORE. We thank Dr. Anatoly Bekkerman and Semion Goberman the Faculty of Chemistry technical team for constructing the photocell; Dr. Guy Ankonina from the PV lab for assistance in design and execution of electrochemical tests; Dr. Nurit Waldman and Dr. Shany Hershkovitz from the hydrogen lab for assistance in quantification of the hydrogen production. We thank Asaf Kay for help with the SEM images. We thank Yaniv Shlosberg, Shmuel Carmeli, and Larisa Panz for their assistance in analysis of the mediator. D.K. and G.Sa. are supported by fellowships of the Nancy & Stephen Grand Technion Energy Program (GTEP). D.K. is supported by fellowships of the Israeli Ministry of Science, Technology and Space. G.Sa. is supported by a Schulich Graduate fellowship.

Author contributions

G.Sa., D.K., A.R., G.Sc. and N.A. conceived the idea. D.K., G.Sa., A.R., G.Sc. and N.A. designed the experiments. G.Sa. and D.K. performed the main experiments. G.Sa., F.C. and F.Z. performed the SECM experiments. T.T. performed part of the cell viability experiments. V.L. performed the immunoblot experiment, S.M., J. S. and A.A. performed metabolomics profiling. A.R., N.A., G.Sc., W.S., F.C., F.Z., G.Sa. and D.K. analyzed the data. A.R., N.A., W.S., F.C., G.Sc., G.Sa. and D.K. wrote the paper. A.R., N.A. and G.Sc. supervised the entire research.

Additional information

Supplementary Information accompanies this paper at <https://doi.org/10.1038/s41467-018-04613-x>.

Competing interests: The authors declare no competing interests.

Reprints and permission information is available online at <http://npg.nature.com/reprintsandpermissions/>

Publisher's note: Springer Nature remains neutral with regard to jurisdictional claims in published maps and institutional affiliations.



Open Access This article is licensed under a Creative Commons Attribution 4.0 International License, which permits use, sharing, adaptation, distribution and reproduction in any medium or format, as long as you give appropriate credit to the original author(s) and the source, provide a link to the Creative Commons license, and indicate if changes were made. The images or other third party material in this article are included in the article's Creative Commons license, unless indicated otherwise in a credit line to the material. If material is not included in the article's Creative Commons license and your intended use is not permitted by statutory regulation or exceeds the permitted use, you will need to obtain permission directly from the copyright holder. To view a copy of this license, visit <http://creativecommons.org/licenses/by/4.0/>.

© The Author(s) 2018